NEW MODEL FOR COMPRESSIVE STRENGTH LOSS OF LIGHTWEIGHT CONCRETE EXPOSED TO ELEVATED TEMPERATURES

by

Ahmet Emin KURTOGLU[a*] ***and Derya BAKBAK***[b]

[a] Department of Civil Engineering, Istanbul Gelisim University, Avcilar, Istanbul, Turkey
[b] The Grand National Assembly of Turkey (TBMM), Cankaya, Ankara, Turkey

Original scientific paper
https://doi.org/10.2298/TSCI181030042K

This study proposes a new model for the residual compressive strength of structural lightweight concrete after exposure to elevated temperatures up to 1000 °C. For this purpose, a database of residual compressive strengths of fire exposed lightweight concrete was compiled from the literature. Database consisted a total number of 289 data points, used for generating training and testing datasets. Symbolic regression was carried out to generate formulations by accounting for various input parameters such as heating rate, cooling regime, target temperature, water content, aggregate type, and aggregate content. Afterwards, predictions of proposed formulation is compared to experimental results. Statistical evaluations verify that the prediction performance of proposed model is quite high.

Key words: *lightweight concrete, high temperature, compressive strength, symbolic regression, modeling*

Introduction

High temperature exposure is one of the most severe conditions to which the structures can be subjected. Physical and mechanical properties of structures such as volume stability, compressive strength and elastic modulus can be deteriorated significantly after fire exposure, resulting in undesirable failures [1-5]. Previous research has shown that various parameters such as peak exposure temperature, concrete type and strength, aggregate type and content have significant effect on the residual properties of concrete after high temperature exposure. High temperature initiates the internal stress caused by dehydration-induced microstructural change. This is generally followed by the separation and spalling of hot surface layers from the cooler interior [6-8].

Structural lightweight aggregate concrete (LWAC) is used in many applications of modern construction due to its advantages over normal concrete such as lower density, allowing to choose smaller cross-sections for load carrying members [9]. The LWAC are usually classified as natural and artificial. Natural type LWAC is produced using aggregates such as pumice, volcanic cinders, diatomite, *etc.*, whereas perlite, expanded clay, shale, *etc.* are used for the production of artificial type LWAC [10]. Structural LWAC has advantages such as lower thermal expansion coefficient, tensile strain capacity and, most importantly, higher strength-to-weight ratio [11, 12].

* Corresponding author, e-mail: aekurtoglu@gelisim.edu.tr

A number of researchers have studied the residual mechanical properties of lightweight concrete subjected to elevated temperatures. Demirel and Gonen [13] carried out tests on the compressive strength and porosity of lightweight concrete with pumice aggregate and silica fume after exposure to elevated temperatures. Sancak *et al.* [14] have investigated the residual properties of fire exposed lightweight concrete incorporating silica fume. Tanyildizi [15] studied the residual compressive and splitting tensile strength of fire exposed lightweight concrete incorporating fly ash and developed a model via fuzzy logic. Tanyildizi and Cevik [16] investigated the mechanical performance of lightweight concrete exposed to high temperature and proposed a model based on genetic programming. They tested the fire exposed lightweight concrete incorporating silica fume for compressive and splitting tensile strengths. Bideci [17] conducted tests to assess the effect of high temperature on lightweight concrete produced using colemanite and cement coated pumice aggregates. Torić *et al.* [18] analyzed the short term mechanical properties of lightweight concrete after temperature exposures up to 600 °C. They also investigated the effect of cooling regime after peak temperature is achieved. Akcaozoglu and Akcaozoglu [19] studied the residual physical and mechanical properties of fire exposed lightweight concrete produced with expanded clay aggregate or calcium aluminate cement, tested using different cooling regimes. Baloch *et al.* [20] studied the residual mechanical properties of fire exposed lightweight concrete incorporating carbon nanotubes.

Predicting the physical and mechanical properties of fire-damaged structures is of significant importance to assess the usability of such structures after exposure to fire. Therefore, there are available models for predicting such properties of concrete exposed to fire exposure. Knaack *et al.* [21] proposed several models depending on the aggregate type, test method and maximum temperature exposure. In this study, the model considered was the one proposed for LWAC and residual test type, which is expressed:

$$\frac{f_{cm}}{f_{cmo}} = \kappa_{f_{m0}} + \kappa_{f_{m1}} T + \kappa_{f_{m2}} T^2 + \kappa_{f_{m3}} T^3 \tag{1}$$

where f_{cm} is the residual compressive strength after exposure to peak temperature, f_{cmo} is the strength at room temperature, and T is the temperature in degrees Fahrenheit. For lightweight concrete and residual test type, κ_{fm0}, κ_{fm1} , κ_{fm2}, and κ_{fm3} are given as 1.037, –5.483e–04, 3.686e–07, and –2.208e–10, respectively.

Despite there are available formulations for modeling the mechanical properties such as compressive strength and elastic modulus of fire-exposed lightweight concrete, these formulations generally do not account for significant contributions of parameters such as aggregate type, heating rate, cooling regime, water content and silica fume or fly ash-incorporated cement content, *etc.* Thus, there is still lack of a unified, explicit and simple-to-use formulation for residual compressive strength of fire-exposed lightweight concrete.

Description of database

A total of 289 data points compiled from eight papers [13-20] were used to develop an empirical formulation for relative compressive strength (f_c/f_{c0}) of lightweight concrete after exposure to high temperatures. Residual test type where the specimen is placed in the furnace after the water curing is completed was used by all eight papers. For the collection of data, followed considerations are: all experiments followed the residual test type, not stressed or unstressed, and lightweight concrete mixtures with fibers are not included.

Figure 1 shows the distribution of compressive strength values at room temperature, f_{c0}, from eight data sources used in this research. Compressive strength at room temperature varies approximately between 16.6-62.6 MPa.

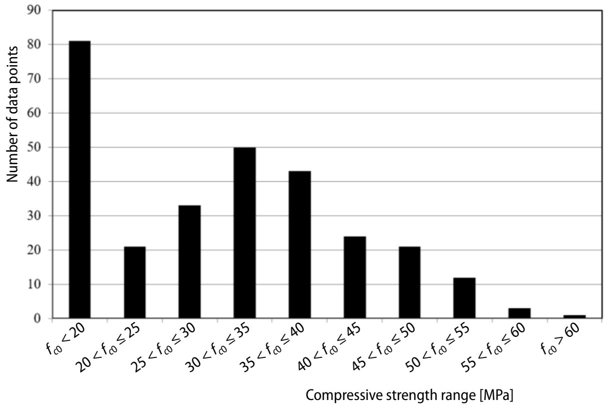

Figure 1. Data distribution for compressive strength at room temperature

Database consist of numeric and non-numeric variables. Non-numeric design variables (*e. g.*, aggregate type and cooling regime) are converted to numeric values. For instance: 1, 2, and 3 are assigned for pumice aggregate, expanded clay aggregate, and expanded shale aggregate, respectively. Similar process is followed for variables of cooling regime, as listed in tab. 1. Some researchers used natural cooling regime where the specimen was removed from the furnace and allowed to cool naturally. Furnace cooling, on the other hand, is based on the cooling of specimen inside the furnace by decreasing the temperature with a specified rate. Some researchers used water cooling where they put the specimen into water tank after the peak temperature exposure is completed.

Table 1. Conversion of non-numeric properties

	Non-numeric designation	Numeric designation
Aggregate type	Pumice	1
	Expanded clay	2
	Expanded shale	3
Cooling regime	Natural	1
	Furnace	2
	Water	3

Table 2 summarizes the data ranges on which the proposed formulation is based. Data includes mixtures with partial replacement of cement with silica fume or fly ash. On the other hand, different sample shapes (cylinder or cubic) and sizes were used. Water curing and total curing durations were also included in the database, as some papers followed a curing regime where they kept the specimens in room temperature after water curing, until a specified day. Heating rate denotes the increase rate of temperature up to desired peak temperature. Target temperature exposure time stand for the duration in which the specimen was exposed to peak temperature, in hours. Mixture properties concrete such as the contents of binder, water, aggregate, superplasticizer and water/cement (W/C) was also included in the database.

Symbolic regression

Symbolic regression is evolutionary computing-based method for exploring the space of mathematical formulations while minimizing numerous error metrics [22].

The symbolic regression algorithm is unlike the traditional regression techniques that are based on parameter-fitting to an equation of a preset structure. Unlike those established regression techniques, symbolic regression searches for the parameters as well as the structure of equations. Random combination of mathematical expressions such as algebraic operators (+, –, ÷, ×), constants, analytical functions (*e. g.*, *sine* and *cosine*) and state variables is utilized to

Table 2. Summary of data and data ranges

Source	[16]	[15]	[18]	[19]	[13]	[14]	[17]	[20]
Data points	96	96	36	12	10	30	4	5
Agg. type	1	1	2	2	1	1	1	3
Spec. grav.	2	2	Not reported	0.43	Not reported	1.926	Not reported	1.36
Water absorption 24 hours [%]	23	23	Not reported	20.1	Not reported	5.83-8.25	Not reported	7.12
Binder	Cement Cement+ Silica fume	Cement Cement+ Fly Ash	Cement Cement+ Silica Fume	Cement	Cement Cement+ Silica Fume	Cement Cement+ Silica Fume	Cement	Cement
Cube/cylinder	Cube 100×100× ×100	Cube 100×100× ×100	Cylinder 75×225	Cube 71×71×71	Cube 100×100× ×100	Cylinder 50×100	Cube 100×100× ×100	Cylinder 100×200
Water curing [days]	28	28	7	60	365	28	28	28
Total curing [days]	28	28	90	120	365	90	28	28
Heating rate [°Cmin^{-1}]	2.5	2.5	2	8	6	5	5	5
Target temp. exposure [hours]	1	1	2.5	1	1	Not reported	1	2.5
Cooling regime	Natural	Natural	Furnace	Natural, Water	Natural	Furnace	Natural	Natural
Temperature [°C]	20-800	20-800	20-600	22-1000	20-1000	20-1000	20-600	23-800
Cement [kgm^{-3}]	280-500	280-500	350-470	400	405-450	387-430	400	297
Silica fume [kgm^{-3}]	0-150	0	0-50	0	0-45	0-43	0	0
Flyash [kgm^{-3}]	0	0-150	0	0	0	0	0	0
Aggregate [kgm^{-3}]	775-1038	780-1038	1024-1160	955	935	1330-1332	1362.48	1097
Water [kgm^{-3}]	308-385	308-385	175-190	200	310-315	187-202	207	148.5-151.5
W/C	0.77-1.1	0.77-1.1	0.40-0.50	0.5	0.68-0.70	0.43-0.47	0.52	0.50-0.51
Superplast [kgm^{-3}]	4.8-6	4.8-6	3.5-4.7	4.88	0-3.6	0-8.6	Not reported	5.94
f_c/f_{c0}	0.13-1.09	0.09-1.09	0.36-1.05	0.23-1.00	0.09-1.00	0-1.03	0.53-1.08	0.38-1.00

generate initial expressions. In the next step, new equations are produced by recombination of former equations and probabilistically changing sub-expressions of produced equations. The equations that fit the experimental data with minimum error are kept and the other solutions are eliminated. The algorithm returns the set of equations that reached to a desired level of accuracy. Although it is possible to use symbolic regression for the purpose of finding explicit [23] and differential equations [24], finding conservation laws and invariant equations using symbolic regression approach may not be as effective [25].

The unary operations (*e. g.*, exp, abs, log) or binary operations (*e. g.*, add, div, mult.) can be used. The operation types can be narrowed down in case some information about the problem is known [26, 27].

The change of operation type (*e. g.* mult. to div.) is possible by mutation in symbolic regression method such as changing an operation argument (*e. g.* change $x+1$ to $x+x$), adding an operation (*e. g.* change $x+x$ to $x + (x*x)$) or deleting an operation (*e. g.*, change $x+x$ to x).

The exchange of sub-trees (or sub-graphs) from two parents can be implemented by crossover function. In order to illustrate it better, this example can be considered: crossing $f_1(x) = x^3 + 3$ and $f_2(x) = x^4 + \cos(x) + x^2$ could produce a child $f_3(x) = x^3 + \cos(x)$. In this example, the leaf node +3 was exchanged with the $\cos(x)$ term [28].

Fitness prediction

Minimization of error on the training set is the main objective of the fitness in symbolic regression [29-32].

For the calculation of error, numerous ways such as squared error, absolute error, log error are available. Despite the fact that the choice of fitness measurement method is not critical, it is known that different metrics work better on different problems. In this paper, we utilize the mean absolute error (MAE) for fitness measurement:

$$\text{fitness}(s) = \frac{1}{N}\sum_{i=1}^{N}\left|s(x_i) - y_i\right| \tag{2}$$

where s is a possible solution (algebraic expression), x_i and y_i are training data input and outputs, and N is the total number of training examples in training data set.

Fitness prediction is considered to be a new method that is applied to determine the performance of different mathematical expressions on explanation of the experimental data more efficiently and optimization of the pressure to fit multiple aspects of data [33, 34]. Figure 2 illustrates solution sizes and bloat for fitness prediction and exact fitness.

Proposed model

Main objective of the current study is to produce an empirical formulation based on symbolic regression, to predict the relative compressive strength (f_c/f_{c0}) of lightweight concrete exposed to high temperatures. The model is produced based on experimental results described in section *Description of database*. For the development of this model, 75% of data is used as training set whereas remaining 25% is used for testing the validity of proposed model. The selection process is implemented on a random basis.

Proposed formulation is given by eq. (3) for the relative strength (f_c/f_{c0}) obtained by symbolic regression modeling.

$$\frac{f_c}{f_{c0}} = k_1 + k_2\, HR\, CL\, T\, W + k_3\, T^2\, W^2 + k_4\, AT\, CL\, T + k_5\, A W T^2 \tag{3}$$

where, HR [°Cmin^{-1}] is heating rate, CL – the cooling regime (defined in tab. 1), T [°C] – the target temperature, W [kgm^{-3}] – the water content, AT – the aggregate type (defined in tab. 1), and A [kgm^{-3}] – the aggregate content. The constants are k_1 = 1.00156, $k_2 = 1.071\cdot10^{-7}$, $k_3 = 2.437\cdot10^{-12}$, k_4 = -0.00013, and $k_5 = -4.0995\cdot10^{-12}$.

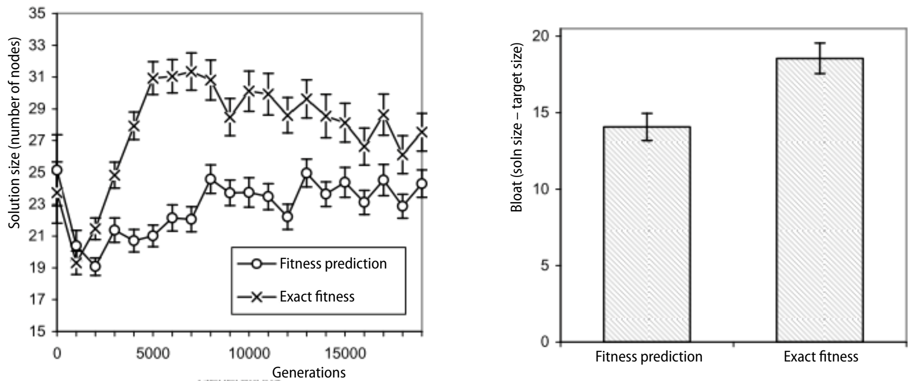

Figure 2. (a) The size of best solution during regression averaged over 100 test runs, (b) total average bloat averaged over 500 randomly generated expressions

Discussion and results

Performance of proposed model

Figure 3 compares the predictions of proposed formulation with that of experimental results for relative compressive strength. As can be observed, compared data points are clustered around a 45° line and the coefficient of determination, R^2, whose mathematical expression is given in eq. (4), is calculated as 0.9508, 0.9274, and 0.944 for training set, testing set and total set, respectively.

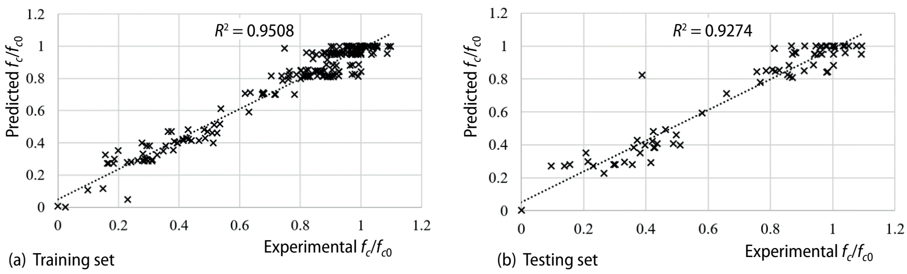

Figure 3. Comparison of experimental and predicted results

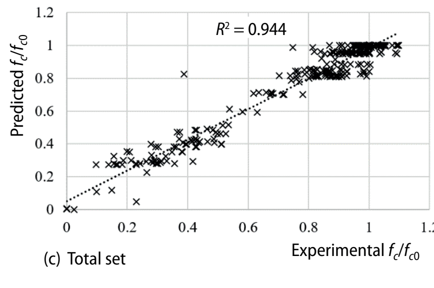

Figure 4 compares the experimental data with the predictions of proposed formulation and Knaack *et al.* [21] model given in eq. (1). As observed, the predicted values generally follow a similar trend with that of experimental dataset.

Model validation

The model was validated through the comparison of statistical results of the predicted values and Knaack *et al.* [21] model. For this purpose, statistical norms, namely as, coefficient of determination, R^2, MAE, mean squared error (MSE) and coefficient of variation (CoV) were used. Mathematical expressions of these norms are given in eqs. (4)-(7).

$$R^2 = 1 - \frac{\sum_{i=1}^{N}(O_i - P_i)^2}{\sum_{i=1}^{N}(O_i - O_{ort.})^2} \tag{4}$$

$$MSE = \frac{\sum_{i=1}^{N}\left(O_i - P_i\right)^2}{N} \tag{5}$$

$$MAE = \frac{1}{N}\sum_{i=1}^{N}\left|O_i - P_i\right| \tag{6}$$

$$CoV = \frac{\sigma}{\overline{X}} \tag{7}$$

where N is the number of data, O_i – the experimental value of i_{th} data, P_i – the predicted value of i_{th} data, σ – the standard deviation, and $\overline{X}$ – the mean value.

As seen in tab. 3, proposed formulation estimates match fairly well with experimental results.

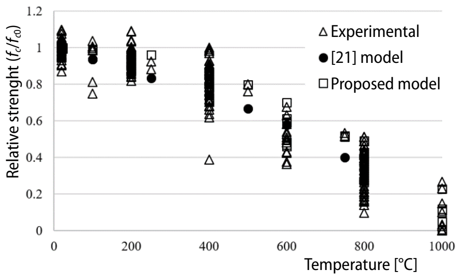

Figure 4. Comparison of proposed model and Knaack *et al.* [21] model

Table 3 Performance of Knaack *et al.* [21] model and proposed model

	[21], eq. (1)	Proposed model, eq. (3)
R^2	0.890	0.944
MAE	0.082	0.049
MSE	0.011	0.005
COV	0.396	0.373

Conclusions

In this study, an empirical model is proposed to predict the relative compressive strength of lightweight concrete with or without partial cement replacement by silica fume/fly ash, after exposure to elevated temperature. Proposed formulation is based on symbolic regression and the used database includes the experiments conducted using residual testing type only. Following conclusions are drawn from the current study:

- Proposed symbolic regression formulation is based on wide range of experimental database provided in this paper. The formulation appears to have high prediction capability, *i. e.*, high R^2 of 94.4% was obtained, which is higher than that of Knaack *et al.* [21] model. Also, other statistical norms such as MAE, MSE, and CoV confirms the superior prediction accuracy of proposed model.
- In addition to the significant effect of peak temperature, proposed model accounts also for the independent parameters such as heating rate, cooling regime, water content, aggregate content and aggregate type, which apparently improves the prediction performance.
- Proposed formulation has the capability to predict residual strength of both cement-only mixture lightweight concrete and silica fume/fly ash based lightweight concrete.
- Symbolic regression is an effective and robust tool for generating easy-to-use predictive models. The findings of this study may lead to the further use of this technique for civil engineering problems in the future.

References

[1] Arioz, O., Retained Properties of Concrete Exposed to High Temperatures: Size Effect, *Fire and Materials: An International Journal*, *33* (2009), 5, pp. 211-222
[2] Fletcher, I. A., *et al.*, Behaviour of Concrete Structures in Fire, *Thermal Sscience*, *11* (2007), 2, pp. 37-52
[3] Georgali, B., Tsakiridis, P., Microstructure of Fire-Damaged Concrete, A Case Study, *Cement and Concrete composites*, *27* (2005), 2, pp. 255-259
[4] Poon, C., *et al.*, Compressive Behavior of Fiber Reinforced High-Performance Concrete Subjected to Elevated Temperatures, *Cement and Concrete Research*, *34* (2004), 12, pp. 2215-2222
[5] Sakr, K., El-Hakim, E., Effect of High Temperature or Fire on Heavy Weight Concrete Properties, *Cement and concrete research*, *35* (2005), 3, pp. 590-596
[6] Chiang, C.-H., Chung-Chia, Y., Artificial Neural Networks in Prediction of Concrete Strength Reduction Due to High Temperature, *ACI Materials Journal*, *102* (2005), 2, pp. 93-102
[7] Lawson, J. R., *et al.*, *Mechanical Properties of High Performance Concrete After Exposure to Elevated Temperatures*, 2000, US Department of Commerce, Technology Administration, National Institute of Standards and Technology, Gaithersburg, Md., USA, 2000
[8] Nassif, A., *et al.*, A New Quantitative Method of Assessing Fire Damage to Concrete Structures, *Magazine of Concrete Research*, *47* (1995), 172, pp. 271-278
[9] Carette, G., *et al.*, Mechanical Properties of Concrete Incorporating High Volumes of Fly Ash From Sources in the US, *Materials Journal*, *90* (1993), 6, pp. 535-544
[10] Uysal, H., *et al.*, The Effects of Different Cement Dosages, Slumps, and Pumice Aggregate Ratios on the Thermal Conductivity and Density of Concrete, *Cement and Concrete Research*, *34* (2004), 5, pp. 845-848
[11] Topcu, I. B., Semi Lightweight Concretes Produced by Volcanic Slags, *Cement and Concrete Research*, *27* (1997), 1, pp. 15-21
[12] Yasar, E., *et al.*, Strength Properties of Lightweight Concrete Made with Basaltic Pumice and Fly Ash, *Materials Letters*, *57* (2003), 15, pp. 2267-2270
[13] Demirel, B., Gonen, T., The Effect of High Temperature on Compressive Strength and Porosity of Carbon Fiber Reinforced Lightweight Concrete (in Turkish), *Pamukkale Universitesi Muhendislik Bilimleri Dergisi*, *14* (2008), 2, pp. 223-228
[14] Sancak, E., *et al.*, Effects of Elevated Temperature on Compressive Strength and Weight Loss of the Light-Weight Concrete with Silica Fume and Superplasticizer, *Cement and Concrete Composites*, *30* (2008), 8, pp. 715-721
[15] Tanyildizi, H., Fuzzy Logic Model for Prediction of Mechanical Properties of Lightweight Concrete Exposed to High Temperature, *Materials & Design*, *30* (2009), 6, pp. 2205-2210
[16] Tanyildizi, H., Cevik, A., Modeling Mechanical Performance of Lightweight Concrete Containing Silica Fume Exposed to High Temperature Using Genetic Programming, *Construction and Building Materials*, *24* (2010), 12, pp. 2612-2618
[17] Bideci, O. S., The Effect of High Temperature on Lightweight Concretes Produced with Colemanite Coated Pumice Aggregates, *Construction and Building Materials*, *113* (2016), June, pp. 631-640
[18] Torić, N., *et al.*, Mechanical Properties of Lightweight Concrete after Fire Exposure, *Structural Concrete*, *17* (2016), 6, pp. 1071-1081
[19] Akcaozoglu, K., Akcaozoglu, S., The Effect of Elevated Temperature on the Lightweight Concrete Produced by Expanded Clay Aggregate and Calcium Aluminate Cement, *Bilge International Journal of Science and Technology Research*, *1*, (2017), 2, pp. 59-70
[20] Baloch, W. L., *et al.*, Effect of Elevated Temperatures on Mechanical Performance of Normal and Lightweight Concretes Reinforced with Carbon Nanotubes, *Fire Technology*, *54* (2018), 5, pp. 1331-1367
[21] Knaack, A. M., *et al.*, Compressive Strength Relationships for Concrete under Elevated Temperatures, *ACI Materials Journal*, *107* (2010), 2, pp. 164-175
[22] Koza, J. R., Genetic Programming as a Means for Programming Computers by Natural Selection, *Statistics and Computing*, *4* (1994), 2, pp. 87-112
[23] Duffy, J., Engle-Warnick, J., Using Symbolic Regression to Infer Strategies From Experimental Data, in: *Evolutionary Computation in Economics and Finance*, (Eds. S.-H., Chen), Springer, New York, USA, 2002, pp. 61-82
[24] Bongard, J., Lipson, H., Automated Reverse Engineering of Nonlinear Dynamical Systems, *Proceedings of the National Academy of Sciences*, *104* (2007), 24, pp. 9943-9948

[25] Schmidt, M., Lipson, H., Distilling Free-Form Natural Laws from Experimental Data, *Science*, *324* (2009), 5923, pp. 81-85
[26] Augusto, D. A., Barbosa, H. J., Symbolic Regression Via Genetic Programming, *Proceedings,* 6th Brazilian Symposium on Neural Networks, Rio de Janeiro, Brazil, 2002, pp. 173-178
[27] Schmidt, M., Lipson, H., Coevolution of Fitness Maximizers and Fitness Predictors, *Proceedings*, GECCO Late Breaking Paper, Washington DC, 2005
[28] Schmidt, M. D., Lipson, H., Learning Noise, *Proceedings,* 9th Annual Conference on Genetic and Evolutionary Computation, London, UK, 2007, pp. 1680-1685
[29] Dolin, B., *et al.*, Co-Evolving an Effective Fitness Sample: Experiments in Symbolic Regression and Distributed Robot Control, *Proceedings,* 2002 ACM symposium on Applied Computing, Madrid, Spain, 2002, pp. 553-559
[30] Eggermont, J., van Hemert, J., Stepwise Adaptation of Weights for Symbolic Regression with Genetic Programming, *Proceedings,* 12th Belgium/Netherlands Conference on Artificial Intelligence (BNAIC'00), Leiden, The Netherlands, 2000, pp. 259-266
[31] Hoai, N. X., *et al.*, Solving the Symbolic Regression Problem with Tree-Adjunct Grammar Guided Genetic Programming: The Comparative Results, *Proceedings,* 2002 Congress on Evolutionary Computation, 2002. CEC'02, IEEE, Honolulu, Hi., USA, 2002, pp. 1326-1331
[32] Keijzer, M., Improving Symbolic Regression with Interval Arithmetic and Linear Scaling, *European Conference on Genetic Programming.*, Essex, UK, 2003, pp. 70-82
[33] Schmidt, M. D., Lipson, H., Coevolution of Fitness Predictors, *IEEE Transactions on Evolutionary Computation, 12* (2008), 6, pp. 736-749
[34] Schmidt, M. D., Lipson, H., Co-Evolving Fitness Predictors for Accelerating Evaluations and Reducing Sampling, (2007), DOI: 10.1007/978-0-387-49650-4_8

Paper submitted: October 30, 2018
Paper revised: November 20, 2018
Paper accepted: January 13, 2019